INVITED TALK

Science and Detectors of the Pierre Auger Observatory

A. Etchegoyen [1,2] *for the Pierre Auger Collaboration*

(1) ITeDA,Instituto de Tecnologías en Detección y Astropartículas
(CNEA, CONICET, UNSAM)
(2) UTN-FRBA

Abstract. The high energy spectrum of cosmic rays presents three distinct traits, the second knee, the ankle, and the GZK cutoff and as such, a thorough understanding of cosmic rays encompasses the study of these three features. It is in the second knee - ankle region where cosmic ray sources change from a galactic origin to an extragalactic one. At the higher cutoff energies, the arrival directions show an anisotropy related to the near extragalactic sky. The Pierre Auger Observatory is currently designed to help to unravel these features by performing both spectrum and composition measurements with unprecedented accuracy. The primary particle type in the second knee - ankle region will be studied both with fluorescence telescopes and muon counters giving the air shower longitudinal profiles and muon contents, respectively.

Resumen. El espectro de rayos cósmicos de altas energías presenta tres rasgos distintivos, la segunda rodilla, el tobillo y el corte GZK y por ende comprender en detalle a estos rayos cósmicos implica el estudio de estas tres características. Es en la zona de la segunda rodilla - tobillo en donde acaece el cambio de fuentes de rayos cósmicos de galácticas a extra galácticas. Por otro lado, en la zona de las energías más altas se detecta anisotropía en la dirección de arribo relacionada con el espacio extragaláctico cercano. El Observatorio Pierre Auger está diseñado para el estudio de estos tres rasgos realizando tanto estudios del espectro como de la composición química de los rayos cósmicos primarios con una precisión sin precedentes. La composición química del primario será estudiada con telescopios de fluorescencia y con contadores de muones obteniéndose así los perfiles longitudinales y los contenidos muónicos de los chubáscos cósmicos.

1. Introduction

The Pierre Auger Observatory was built to detect the highest energy cosmic rays known in nature with two distinctive design features, a large size and a hybrid detection system in an effort to detect a large number of events per year with minimum systematic uncertainties. The southern component of the Auger Observatory is located in the west of Argentina, in the Province of Mendoza where it spans an area of 3000 km^2 covered with 1600 water Cherenkov detectors (SD,

surface detectors) deployed on a 1500 m triangular grid with four buildings on the array periphery lodging six fluorescence telescope systems (FD, fluorescence detectors) each one with a $30° \times 30°$ elevation and azimuth field of view (Abraham et al. (2004, 2008a)). With such a geometry, the Observatory has been able to cast light on two spectral features (Abraham et al. (2009a)) at the highest energies, the ankle and the GZK-cutoff (Greisen (1966), Zatsepin et al. (1966)).

The ankle refers to a break in the spectrum which is found at $\sim 10^{18.6}$ eV. by the Auger Observatory. The GZK-cutoff (named after Greisen, Zatsepin, and Kuz'min who suggested it) is a suppression of the cosmic ray flux at very high energies which is reported at $\sim 10^{19.5}$ eV (Abraham et al. (2009a)). This suppression is pertinent to the reported anisotropy in the arrival directions of cosmic rays with energies above $\sim 6 \times 10^{19}$ eV (Abraham et al. (2008b)). This anisotropy may open a new window in astronomy research, charged-particle source identification, since the very high primary-particle energies might permit to trace back the arrival directions and find the cosmic sources. At lower energies the electromagnetic fields deflect charged-particle trajectories rendering impossible to identify the sources, but still composition studies should help to discriminate whether the sources are galactic or extragalactic and the energy region where the transition occurs. Also, non-charged particles (e.g. neutrons and photons) might produce detectable point-like galactic anisotropies. Neutrons with energies above ~ 1.0 EeV could arrive from the galactic-center region without decaying. Photon-induced anisotropies would be easier to identify with the Auger Observatory enhancements (see below) for instance with muon counters, because photon showers have a vanishing muon content.

The cosmic ray spectrum presents a further feature at lower energy named the knee ($\sim 4 \times 10^{15}$ eV), outside the energy region of the Auger Observatory. The knee has been interpreted (Aglietta et al. (2004), Antoni et al. (2005), Kampert et al. (2008)) as the spectrum region where galactic sources fail to accelerate lighter elements to higher energies and only do so to heavier elements. Still and as the energy increases, the number of galactic sources capable of accelerating even the heavier elements will diminish and therefore a transition from galactic to extragalactic sources will take place. This transition is assumed to occur either at the second knee (Nagano et al. (1984), Abu-Zayyad et al. (2001), Pravdin et al. (2003), Abbasi et al. (2004)) or at the ankle (Ave et al. (2001), Pravdin et al. (2003), Abbasi et al. (2004)) and the way to help to identify it would be a change in the cosmic ray composition. Within the Auger baseline design described above, the surface array is fully efficient above $\sim 3 \times 10^{18}$ eV and in the hybrid mode this range is extended down to $\sim 10^{18}$ eV which does not suffice to cover the second knee - ankle region. For this purpose, Auger has two enhancements: AMIGA ("Auger Muons and Infill for the Ground Array") (Etchegoyen et al. (2007), Platino et al. (2009), Buchholtz et al. (2009), Medina-Tanco et al. (2009)) and HEAT ("High Elevation Auger Telescopes") (Klages et al. (2007), Kleifges et al. (2009)). AMIGA is being deployed over a small area of 23.5 km^2 (see Fig. 1) since the cosmic ray flux abruptly increases with diminishing impinging energy. On the other hand, the detectors have to be deployed at shorter distances among each other in a denser array since lower energies imply smaller air shower footprints on the ground. Also, telescopes need to have a higher elevation field of view (FOV) since these showers would develop earlier in the atmosphere.
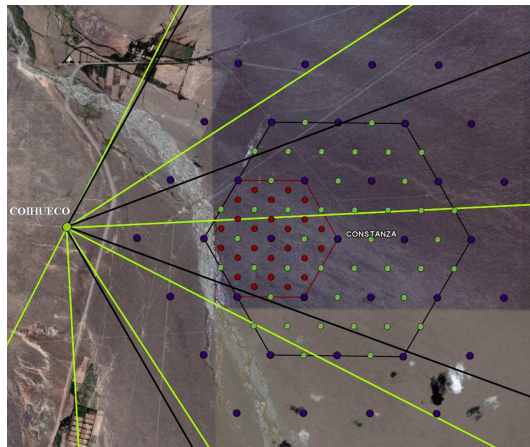
Figure 1.   Auger enhancements layout. Green lines limit the $0° - 30° \times 0° - 30°$ elevation and azimuth FOV of the original 6 telescopes on Cerro Coihueco and the black lines the $30° - 60° \times 0° - 30°$ FOV for the 3 HEAT telescopes. The two hexagons limit the AMIGA infilled areas of 5.9 and 23.5 km^2 with 433 and 750 m triangular grid detector spacings, respectively. Each dot within these hexagons represents a pair of a water Cherenkov detector and a muon counter. The center dot, named Constanza, is placed ~ 6.0 away from Cerro Coihueco.

2.   Spectrum, anisotropy, and composition

The Auger Observatory as already mentioned has a hybrid detection system composed of SD and FD systems. The SD array has a flat exposure determined by the array geometry, a 100% duty cycle and a $\geq 1°$ arrival directions uncertainty. Its energy assignment depends on simulations which assume a hadronic model and a primary composition. A hybrid measurement is performed when an FD system and at least a SD station are triggered. This combined time measurement improves the arrival direction reconstruction to $\geq 0.2°$. The energy assignment is performed by integration of the longitudinal profile rendering a calibration quite independent from both model and composition. Still, the hybrid (or FD) exposure increases with energy and it only has a $\sim 10\%$ duty cycle. The hybrid energy calibration has several systematic uncertainties (fluorescence yield, absolute calibration, atmospheric attenuation, and reconstruction method) which have been estimated to give an overall energy resolution of $\Delta E/E \sim 22\%$. The Auger Collaboration calibrates the SD array with hybrid events in order to avoid any dependence on simulations. The procedure follows four steps: i) the lateral profile is fitted with a carefully chosen lateral distribution function and the signal, S(1000), at a core distance of 1000 m is extracted, see Fig.2.lhs, ii) the difference in signal attenuation due to different atmospheric depths traversed is experimentally corrected by renormalizing the signal to the signal the shower would have produced with an arrival angle of $38°$, see Fig.2.rhs, iii) the shower energy is evaluated from the longitudinal profile measured by the FD system, see Fig.3.lhs, and iv) the calibration curve is obtained by plotting lg(S$_{38}$) vs lg(E$_{FD}$), see Fig.3.rhs.
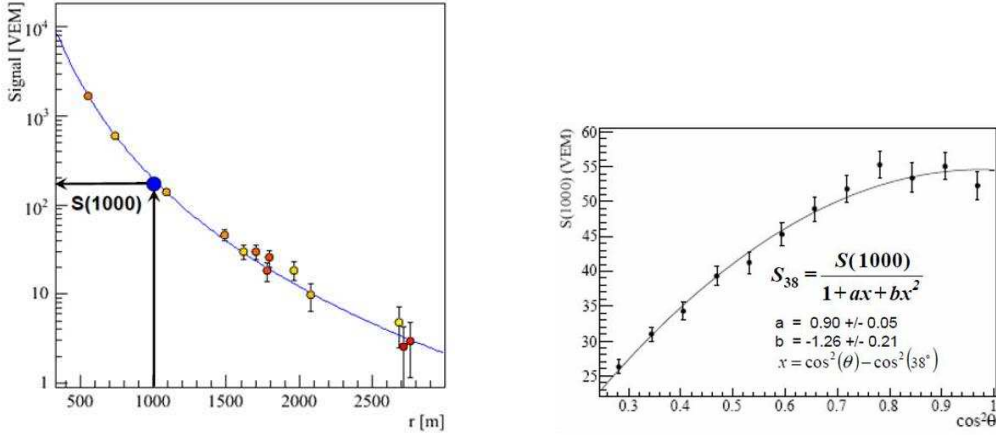
Figure 2.   *(lhs)* Shower lateral profile; *(rhs)* Shower attenuation curve.
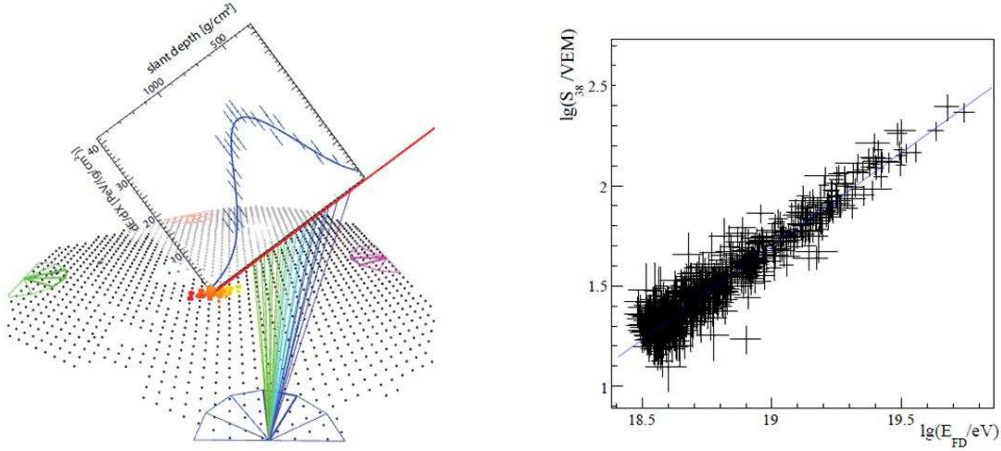

Figure 3.   *(lhs)* Shower longitudinal profile; *(rhs)* Energy calibration curve.

With the above mentioned calibration, the spectrum of cosmic rays can be obtained with the large number of events measured by the 100% duty cycle SD array. But the SD array is fully efficient for $E \geq 3 \times 10^{18}$ eV while the hybrid system from $E \geq 10^{18}$ eV and therefore the total spectrum can be measured from this latter energy onwards. Details on the event selection and applied quality cuts can be seen in (Abraham et al. (2009a)). The measured flux versus primary energy is displayed in Fig.4 for both hybrid and SD detections (the flux is multiplied by E^3 in order to highlight the ankle and the cutoff features). It is clearly seen that both data sets give quite consistent results, no systematic deviations in neither flux nor energy. The ankle is seen at $\sim 10^{18.6}$ eV and the GZK-cutoff at $\sim 10^{19.5}$ eV (Abraham et al. (2009a)). Both are clear and notorious features, the spectrum is reaching its end.

The cutoff is consistent with the predicted energy loss by the interaction of extragalactic cosmic rays with the microwave background radiation (Greisen
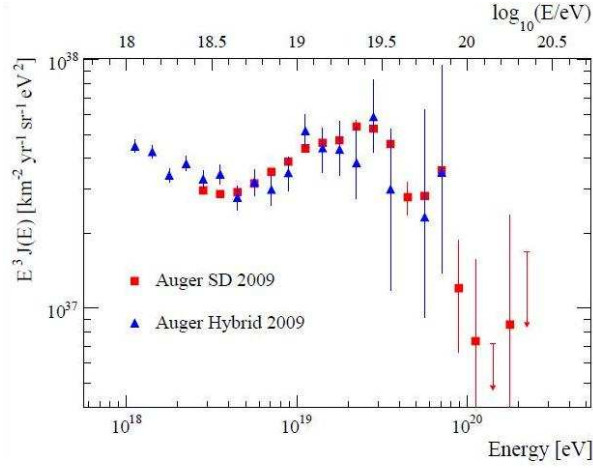
Figure 4.   Auger spectrum

(1966), Zatsepin et al. (1966)). Also, this process will favor proton or iron primaries from the nearby universe (see Fig.5).
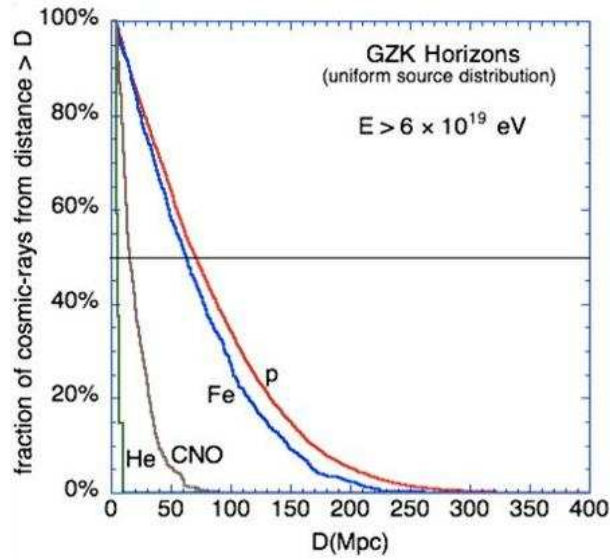

Figure 5.   GZK horizons, only Fe and p may survive $D \geq 100$ Mpc, other nuclei will rapidly disappear for $D \geq 20$ Mpc.

Anisotropy in the arrival directions of above the cutoff ($\sim 10^{18.6}$ eV) may appear since the GZK energy loss process confines the possible cosmic rays sources to only a few in the nearby universe. This feature opens the possibility to detect such sources for their posterior study opening a field of novel astronomy, charged-particles astronomy. A first anisotropy search was published (Abraham et al. (2008b)) for cosmic rays with $E \geq 55$ EeV and a comparison was per-

formed with the positions of AGN galaxies listed in the Véron-Cetty and Véron (VCV) catalogue. The search was performed for AGN within 75 Mpc with circles of radius $3.1°$ around the AGN. The current data set (Hague et al. (2009)) is composed of 58 events with 26 events correlating with nearby AGNs. The probability that an isotropic distribution would by chance mimic these numbers is at the level of 1%. Note also, that the VCV catalogue is incomplete and inhomogeneous, particularly near the galactic plane, and if events were removed with galactic latitude $|b| < 12°$ the correlation becomes 25 out of 45 thus increasing the departure from an isotropic distribution.

An interesting feature is that the region with the largest over density is close to Cen A (an AGN only $\sim 3.5 Mpc$ away) from where 12 events are detected within $18°$ while only 2.7 are expected from isotropy, i.e. a 2% chance probability.

The chemical composition of primaries is of fundamental and unique importance to understand cosmic ray sources. Actually, efforts are concentrated in studying composition changes rather than absolute composition since the latter would be quite dependent on hadronic interaction models (see limits in Fig. 6) and would rely on comparisons to air shower simulations. A usual way to assess composition is by measuring the average depths of shower maximum, X_{max} (and their fluctuations) which are obtained from the air shower longitudinal profiles observed by the fluorescence telescopes (Bellido et al. (2009), Abraham et al. (2009b)).
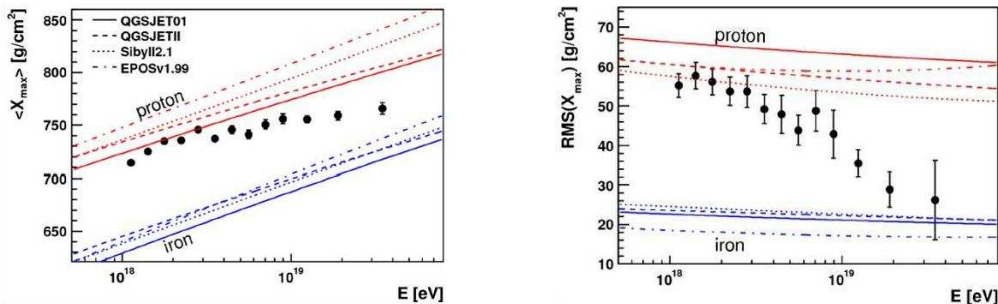

Figure 6.   *(lhs)* Elongation rate (average atmospheric depth of shower maximum versus primary energy); *(rhs)* Average RMS(X_{max}) versus primary energy.

Fig. 6 displays the composition studies performed with Auger hybrid data. There is an indication both in the elongation rate and in X_{max} fluctuations that primaries become heavier with energy (assuming the hadronic interaction does not significantly change in the energy range of interest). The elongation rate was satisfactory fitted (Abraham et al. (2009b)) with two slopes and the break was found at $\sim 10^{18.25}$ eV, a factor of ~ 2 below the reported ankle. These results disagree with those found by the combined data from a hybrid experiment (HiRes/MIA), and the HiRes stereo fluorescence experiment, which overlap by only $\sim 1/4$ of a decade in energy (Sokolsky et al. (2005)). HiRes observes that the composition gets lighter and remains so starting at energies close to the second knee.

3. Auger Observatory Enhancements

As already mentioned the cosmic ray flux shows three high-energy features, the second knee, the ankle and the GZK cutoff. There are currently no doubts about the existence of these three traits, but the understanding of the first two is yet under scrutiny with conflicting results as shown in the previous section. To fully cover this energy region with a single Observatory the Auger Collaboration is building two enhancements, HEAT and AMIGA (Klages et al. (2007), Kleifges et al. (2009), Medina et al. (2006), Etchegoyen (2007), Supanitsky et al. (2008), Platino et al. (2009), Buchholtz et al. (2009), Medina-Tanco et al.(2009)). These enhancements will have an enlarged energy range down to 10^{17} eV and therefore will allow for a good comparison with Kascade-Grande results (Haungs et al. (2009)) whose primary objectives are to study the cosmic ray primary composition and the hadronic interactions in the energy range $10^{16} - 10^{18}$ eV. Fig. 7 shows the HEAT telescopes enclosures and a reconstructed longitudinal profile of a low energy event.
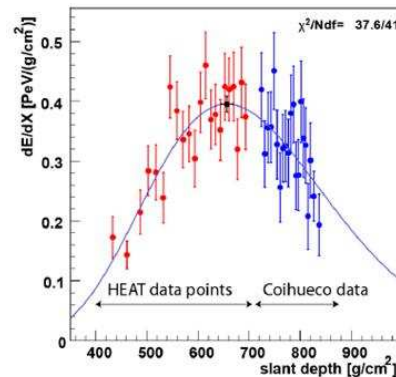

Figure 7.   (Kleifges et al. (2009))*(lhs)* The three buildings of the HEAT telescopes at Cerro Coihueco; *(rhs)* Longitudinal shower profile where both HEAT and Coihueco telescopes are needed in order to reconstruct the profile, event energy $(2.0 \pm 0.2)10^{17}$ eV.

AMIGA data acquisition has started with the SD 750 m infilled area and preliminary analyzes have already been performed with a data set restricted to events with zenith angle $\theta \leq 60°$ and well contained within the infill (i.e. with the six SDs of the hexagon enclosing the highest signal SD in its center active). Preliminary tests were performed reconstructing events with and without the SDs from the infilled area in order to probe the main array reconstruction uncertainties (Platino et al. (2009)). Emphasis was also focused on the preliminary energy calibration by relating the ground signal at 600 m from the core, S(600), with the energy measured by FD (note that the ground signal is taken at 600 m rather than 1000 m since the array spacings are different) (Platino et al. (2009)).

Apart from the extended energy range, the enhancements include muon counters for composition analyses buried alongside each surface detector of the infilled area. Each muon counter has an area of 30 m^2 and it is made of scintillator strips with glued optical fibers (doped with wave length shifters) in a

groove coated on top with a reflective foil. The strips are 1 cm thick and 4.1 cm wide. The counters of the Unitary Cell(an hexagon with 7 detector pairs, one in each hexagon vertex and one in the center) are composed of 4 modules each, 2×5 m^2 and 2×10 m^2 with 2 and 4 m long strips, respectively. Each module has a 64 pixel Hamamatsu H8804MOD photomultiplier tube with a 2 mm $\times$ 2 mm pixel size. The front end bandwidth is of 180 MHz, the electronics sampling is performed at 320 MSps (3.125 ns) with a memory to store up to 6 ms of data. The total number of independent electronic channels per counter is 256 due to the high segmentation requirement in an effort to measure no more than a single muon por segment per unit time. The first fully equipped 5 m^2 module has been designed, built, tested, and buried at the Observatory site, see Fig.8.

Figure 8.   *(lhs)* First module buried at the Observatory site, the insert shows the electronics inside its enclosure; *(rhs)* Muon counter placed over sand bed with service pipe installed, about to be buried.

The extension of Auger to full efficiency down to 0.1 EeV with a direct measure of both X$_{max}$ and shower muon contents will open an unique experimental tool to study the cosmic ray spectrum in the second knee - ankle region, where the transition from galactic to extragalactic sources is assumed to occur. Data with unprecedented precision will be available and in particular there will be a triple hybrid data set (fluorescence, muon, and surface detector detections) on which careful primary energy and composition analyses could be performed.

In conclusion, the Auger Observatory has measured the high energy cosmic ray spectrum and clearly identified the ankle and the cutoff, also it found clear indications of anisotropy in the arrival directions of cosmic rays with energies above 55 EeV. Statistical composition analyses have been performed with depths at shower maximum and their fluctuations. Enhancements are well under way in order to study the transition region from galactic to extragalactic sources with surface, telescope, and muon detectors with unitary efficiencies unbiased in composition.

References

T. Abu-Zayyad et al., 2001, Astrophys. J 557, 686.
Antoni et al., 2005, Astropart. Phys. 24, 1.

J.D. Hague for the Pierre Auger Collaboration, 2009, Proc. 31st ICRC (Lodz, Poland), #0143.

The Auger Collaboration (J.Abraham et al.), 2004, Nucl. Inst. & Meth. A532, 50, 95.

The Auger Collaboration (J.Abraham et al.), 2008a, Nucl. Inst. & Meth. A586, 409, 420.

The Auger Collaboration (J. Abraham et al.), 2008b, Astropart. Phys. 29, 188, 204.

The Auger Collaboration (J. Abraham et al.), submitted to Physics Letters, (2009a).

The Auger Collaboration, submitted to Phys. Rev. Lett., (2009b).

M. Ave et al., 2001, Proc. 27th ICRC (Hamburg), 381.

J. A. Bellido, for the Pierre Auger Collaboration, 2009, Proc. 31st ICRC (Lodz, Poland), #0124.

P.Buchholtz for the Pierre Auger Collaboration, 2009, Proc. 31st ICRC (Lodz, Poland), #0043

The EAS-TOP and MACRO Collaborations (M. Aglietta et al.), 2004, Astropart. Phys. 20, 641.

A. Etchegoyen for the Pierre Auger Collaboration, 2007, Proc. 30th ICRC (Mérida-México), #1307.

Greisen K., 1966, Phys. Rev. Lett. 16, 748.

The HiRes Collaboration (R.U. Abbasi et al.), 2004, Phys. Rev. Lett. 92, 151101.

The Kascade Collaboration (K.H. Kampert et al), 2008, arXiv:astro-ph/0405608.

The Kascade-Grande Collaboration (A. Haungs et al.), 2009, Proc. 31st ICRC (Lodz, Poland), #0401.

H. Klages for the Pierre Auger Collaboration, 2007, Proc. 30th ICRC (Mérida-México), #0065.

M. Kleifges for the Pierre Auger Collaboration, 2009, Proc. 31st ICRC (Lodz, Poland), #0410.

M.C. Medina et. al., 2006, Nucl. Inst. and Meth. A566, 302, 311, and astro-ph0607115.

G. Medina-Tanco for the Pierre Auger Collaboration, 2009, Proc. 31st ICRC (Lodz, Poland), #0137

M. Nagano et al., 1984, J. Phys. G 10, 1295.

M. Platino for the Pierre Auger Collaboration, 2009, Proc. 31st ICRC (Lodz, Poland), #0184.

M.I. Pravdin et al., 2003, Proc. 28th ICRC (Tuskuba), 389.

P. Sokolsky, John Beltz, and the HiRes Collaboration, 2005, Proc. 29th ICRC (Pune, India), 101, 104.

A.D. Supanitsky et al., 2008, Astroparticle Physics 29, 461, 7470.

Zatsepin G. T., Kuzmin V. A., 1966, Sov. Phys. JETP Lett. 4, 78.